LA-3450

LOS ALAMOS SCIENTIFIC LABORATORY
of the
University of California
LOS ALAMOS • NEW MEXICO

The Two-Dimensional Hydrodynamic Hot Spot

Volume III

CIC-14 REPORT COLLECTION
REPRODUCTION
COPY

UNITED STATES
ATOMIC ENERGY COMMISSION
CONTRACT W-7405-ENG. 36

This report expresses the opinions of the author or authors and does not necessarily reflect the opinions or views of the Los Alamos Scientific Laboratory.

Printed in USA. Price $2.00. Available from the Clearinghouse for Federal Scientific and Technical Information, National Bureau of Standards, United States Department of Commerce, Springfield, Virginia

LA-3450
UC-4, CHEMISTRY
TID-4500

LOS ALAMOS SCIENTIFIC LABORATORY
of the
University of California
LOS ALAMOS • NEW MEXICO

Report written: January 5, 1966
Report distributed: April 5, 1966

The Two-Dimensional Hydrodynamic Hot Spot
Volume III

by

Charles L. Mader

ABSTRACT

The shock interactions formed in nitromethane by corners of Plexiglas, aluminum, and gold; the resulting formation of a hot spot; and the buildup to propagating detonation are computed using a high-resolution, Lagrangian, two-dimensional, numerical hydrodynamic code with an Arrhenius rate law and accurate equations of state. Excellent agreement is obtained with the corresponding experimental results.

ACKNOWLEDGMENTS

The author gratefully acknowledges the assistance and contributions of S. R. Orr of T-5, F. H. Harlow, Jr., of T-3, and of J. R. Travis, W. C. Davis, D. Venable, W. Gage, and L. C. Smith of GMX Division of the Los Alamos Scientific Laboratory.

CONTENTS

FIGURES

I. INTRODUCTION

To increase our understanding of the basic processes involved in the shock initiation of inhomogeneous explosives we have studied theoretically the formation of hot spots from shocks interacting with various density discontinuities. In LA-3077[1] we described the hot spots formed when a shock in nitromethane interacts with a spherical void. In LA-3235[2] we described the hot spots formed when a shock in nitromethane interacts with cylindrical or conical voids and with cylinders and spheres of aluminum. These reports were combined and published as reference 3. The PIC (Particle-In-Cell) method for numerically solving the hydrodynamics was used. As described in LA-3235[2] the PIC type of numerical hydrodynamics is not sufficiently detailed to describe the formation of the low-temperature hot spots formed when shocks interact with corners. Therefore we developed a high-resolution (62,000 cells), two-dimensional, Lagrangian hydrodynamic code for solving the problem of initiation at corners. The method is described in detail in Appendix A. The equation of state used is described in detail in Appendix B.

Travis[4] has determined experimentally the shock-induction times for nitromethane-filled corners of various types. We have studied theoretically the corresponding problems for the corners formed by the intersection of a Plexiglas, aluminum, or gold plate with a Plexiglas plate, since they represent the more interesting examples, and found that our computed results reproduced Travis' experimental results.

II. THE FORMATION OF HOT SPOTS AT CORNERS

The problems we are concerned with in this report are exemplified by a plane, piston-supported, flat-topped shock normally incident upon one side (which we have taken as the bottom) of a cubical, liquid-filled box of semi-infinite extent. The corner is formed by the bottom and one of the vertical sides of the box. The problem thus becomes a two-dimensional one describable in the Cartesian coordinates X and Z.

As long as the extensions of the boundaries are infinite, a

description of the hot spot at a given time may be scaled as X/t and Z/t to any other time, t, until a signal returns from a boundary. Therefore, we can obtain increased numerical resolution of the hot spot by allowing the problem to run until a boundary is reached and then scaling the result as desired. For the hot spots described in this report, we had about 1000 cells in the region of the nitromethane hot spot.

A. Plexiglas Corner

Figure 1 shows the interface positions and the isobars for the interaction of a 96-kbar shock (shock velocity U_s = 0.50 cm/μsec, particle velocity U_p = 0.163 cm/μsec) with a nitromethane-filled corner of Plexiglas. The plane-wave-matched nitromethane pressure is 87.6 kbar (U_s = 0.448, U_p = 0.174, T_H = 1180°K). If the distance units in Figure 1 are centimeters, then the time since the shock arrived at the nitromethane/Plexiglas interface is 0.85 μsec. The time since the piston started to move at full velocity is 3.35 μsec. The shock moves faster in the Plexiglas than in the nitromethane, and multiple shocking of the nitromethane occurs. The hot spot isotherms are shown in Figure 2. The nitromethane hot spot has small regions that are 70° hotter than the bulk of the nitromethane. Since the hottest region is near the shock front and is soon cooled by the flow, the determination of an induction time is a complicated problem that must be solved numerically. The hot spot isobars are shown in Figure 3. The nitromethane hot spot has regions that have a pressure 7 kbar higher than the pressure in the bulk of the nitromethane.

B. Aluminum-Plexiglas Corner

Figure 4 shows the interface positions and the isobars for the interaction of a 96-kbar shock in Plexiglas with a nitromethane-filled corner formed by an aluminum plate perpendicular to a Plexiglas plate. The plane-wave-matched aluminum pressure is 162 kbar (U_s = 0.655, U_p = 0.089). The plane-wave-matched nitromethane pressure is 87.6 kbar (U_s = 0.448, U_p = 0.174, T_H = 1180°K). If the distance units in Figure 4 are centimeters, then the time since the shock arrived at the nitro-

methane/Plexiglas or aluminum/Plexiglas interface is 0.85 μsec. The shock moves considerably faster in the aluminum than in the nitromethane, and multiple shocking of the nitromethane occurs. The hot spot isotherms are shown in Figure 5. The nitromethane hot spot has small regions that are 260° hotter than the bulk of the nitromethane. The hot spot isobars are shown in Figure 6. The nitromethane hot spot has regions that have a pressure 27 kbar higher than the pressure in the bulk of the nitromethane.

C. Gold-Plexiglas Corner

Figure 7 shows the interface positions and the isobars for the interaction of a 96-kbar shock in Plexiglas with a nitromethane-filled corner formed by a gold plate perpendicular to a Plexiglas plate. The plane-wave-matched gold pressure is 261 kbar (U_s = 0.365, U_p = 0.037). As before, the plane-wave-matched nitromethane pressure is 87.6 kbar (U_s = 0.448, U_p = 0.174, T_H = 1180°K). If the distance units in Figure 7 are centimeters, then the time since the shock arrived at the nitromethane/Plexiglas or gold/Plexiglas interface is 0.85 μsec. The shock moves slower in the gold than in the nitromethane, and multiple shocking of the nitromethane occurs. The hot spot isotherms are shown in Figure 8. The nitromethane hot spot has regions that are 170° hotter than the bulk of the nitromethane. The hot spot isobars are shown in Figure 9. The nitromethane hot spot has regions that have a pressure 20 kbar higher than the pressure in the bulk of the nitromethane.

All Lagrangian numerical schemes for solving two-dimensional hydrodynamic problems become less accurate the more distorted the mesh. Serious distortion of the mesh occurs in the gold corner problem, and we therefore have a less accurate and less detailed description of the hot spot formed at a gold corner.

III. THE REACTIVE FLOW CALCULATIONS

We calculated the induction times for explosion when shocks interact with corners by repeating the previously described calculations

with chemical reaction permitted. The computed and normalized experimental induction times (obtained by dividing the induction time for detonation at the discontinuity by the induction time for detonation in the surrounding plane-shocked region) of Travis[4] are shown in the following table. Since the computed induction time of nitromethane plane-shocked to 87.6 kbar was 1 ± 0.05 μsec, the computed induction times obtained at discontinuities are automatically normalized, and the computed and experimental times may be compared directly.

System	Calculated Induction Time (μsec)	Normalized Experimental Induction Time (μsec)
Plexiglas Corner	0.6 ± 0.1	0.46
Aluminum-Plexiglas Corner	0.057 ± 0.01	0.05
Gold-Plexiglas Corner	0.12 ± 0.02	0.16

The remarkable agreement obtained between the experimental and theoretical induction times increases our confidence in the accuracy of the theoretical description of the hot spots.

IV. INTERACTION OF A SHOCK WITH A WATER-FILLED CORNER OF PLEXIGLAS

Venable has taken "Phermex" radiographs of the interaction of a 188-kbar shock with a water-filled corner in Plexiglas. The corner was formed by cutting a slot 3 inches deep and 2.5 inches wide in a 4-inch block of Plexiglas. To increase the radiographic resolution, zinc iodide (60 gm) was added to the water (450 gm).

A print of the radiograph, taken 5.5 μsec after the shock reached the bottom of the Plexiglas block, is shown in Figure 10. The computed interface position and isobars are shown in Figure 11. The experimentally observed flow is described well by the calculations, and, in particular, neither calculation nor experiment contains evidence of any jetting at the corner.

V. CONCLUSIONS

The shock interactions formed in nitromethane by corners of Plexiglas, aluminum, and gold; the resulting formation of a hot spot; and the buildup to propagating detonation have been computed. The accuracy of the results was demonstrated by the agreement obtained with the experimental induction times of Travis and the radiographs of Venable.

Since the interaction of shocks with density discontinuities as simple as corners results in a very complicated fluid flow, it appears that detailed numerical studies are essential for an understanding of the experimental results of more complicated systems.

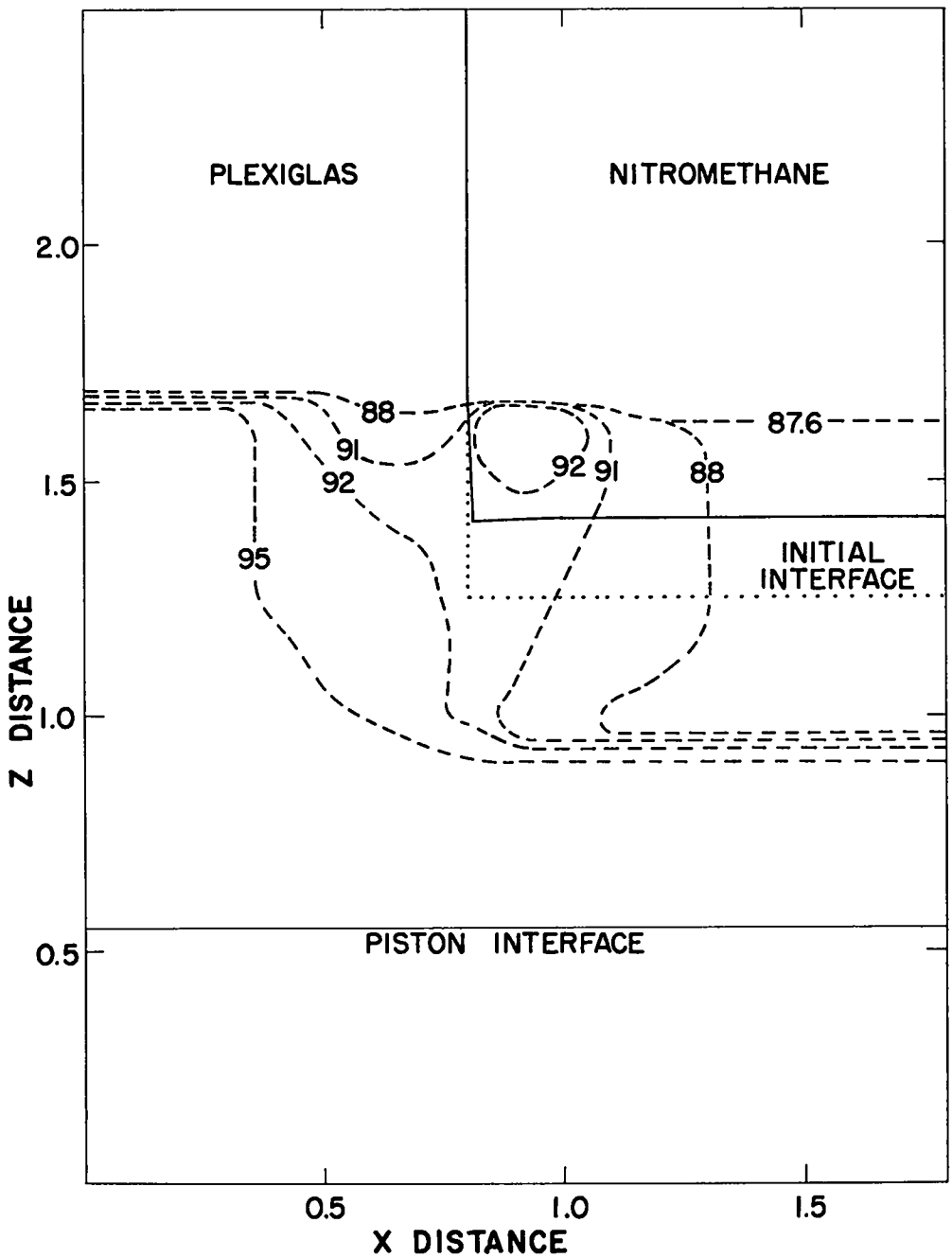

Fig. 1. The interface positions and isobars for the interaction of a 96-kbar shock in Plexiglas with a nitromethane-filled corner of Plexiglas. The interface position is shown by a solid line. The initial interface position is shown by a dotted line. The isobars are shown by dashed lines, and the units are kbars.

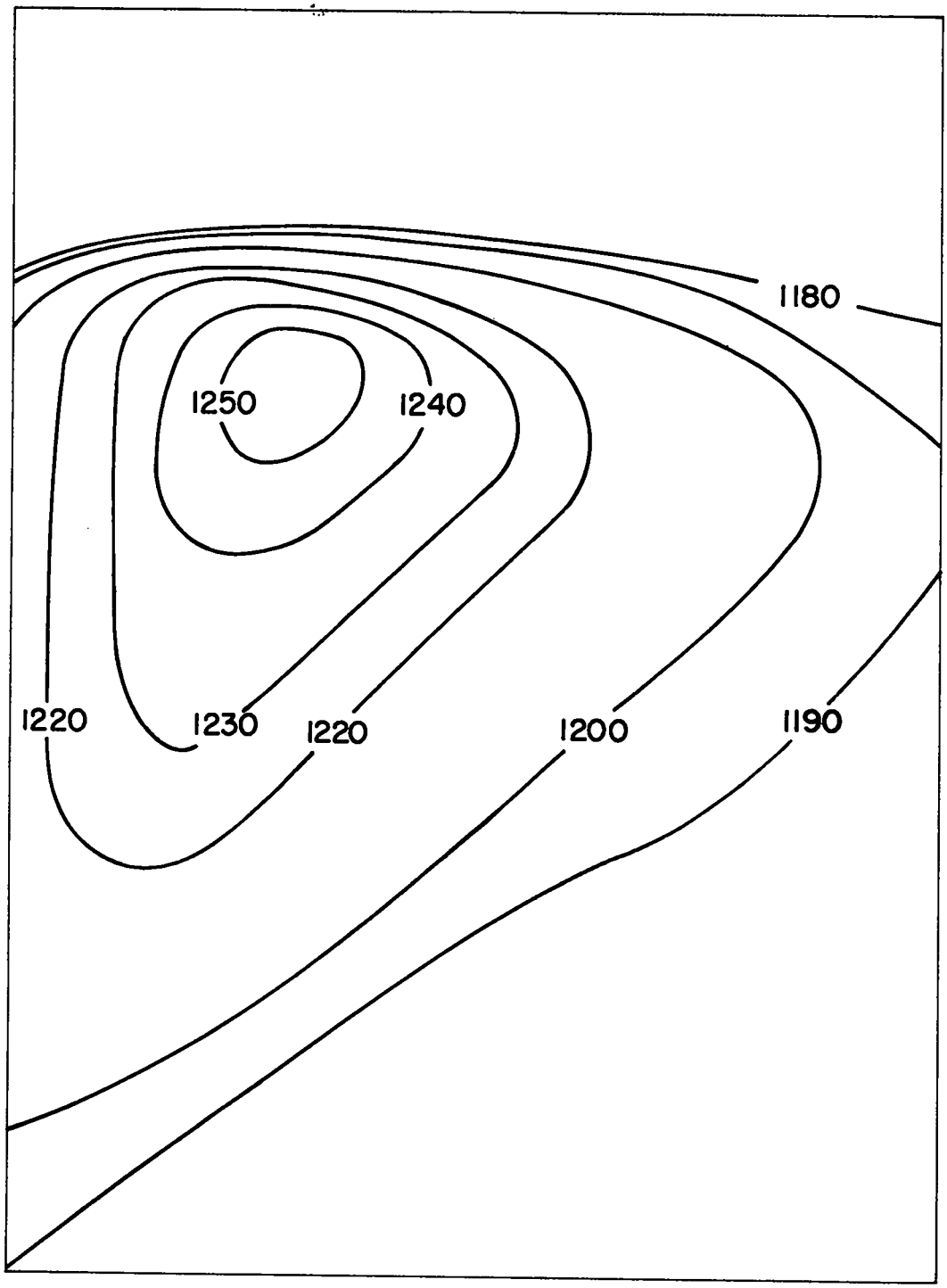

Fig. 2. The hot spot isotherms for the hot spot formed upon the interaction of a 96-kbar shock with a nitromethane-filled corner of Plexiglas. The units are °K.

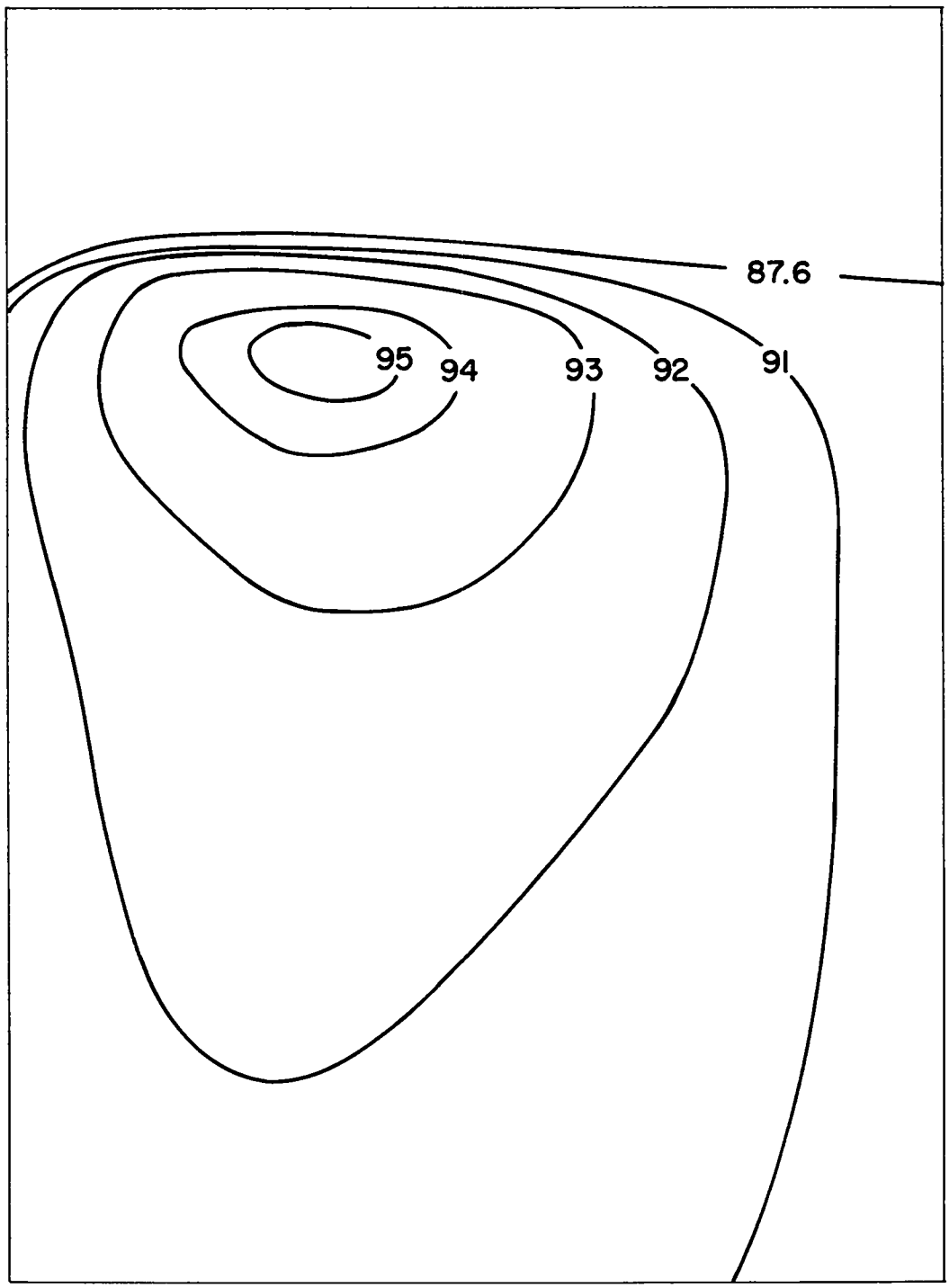

Fig. 3. The hot spot isobars for the hot spot formed upon the interaction of a 96-kbar shock with a nitromethane-filled corner of Plexiglas. The units are kbars.

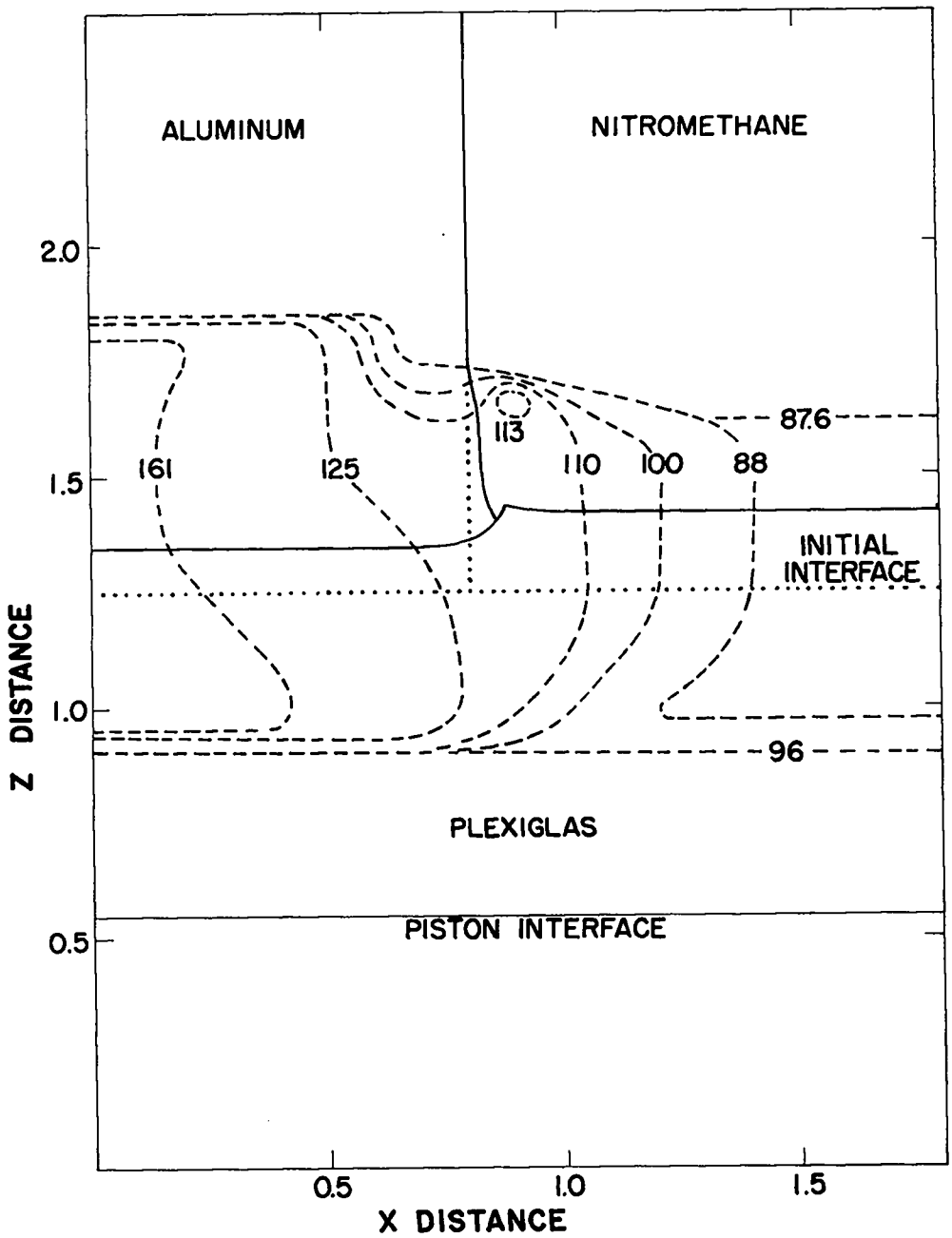

Fig. 4. The interface positions and isobars for the interaction of a 96-kbar shock in Plexiglas with a nitromethane-filled corner formed by an aluminum plate perpendicular to a Plexiglas plate. The interface position is shown by a solid line. The initial interface position is shown by a dotted line. The isobars are shown by dashed lines, and the units are kbars.

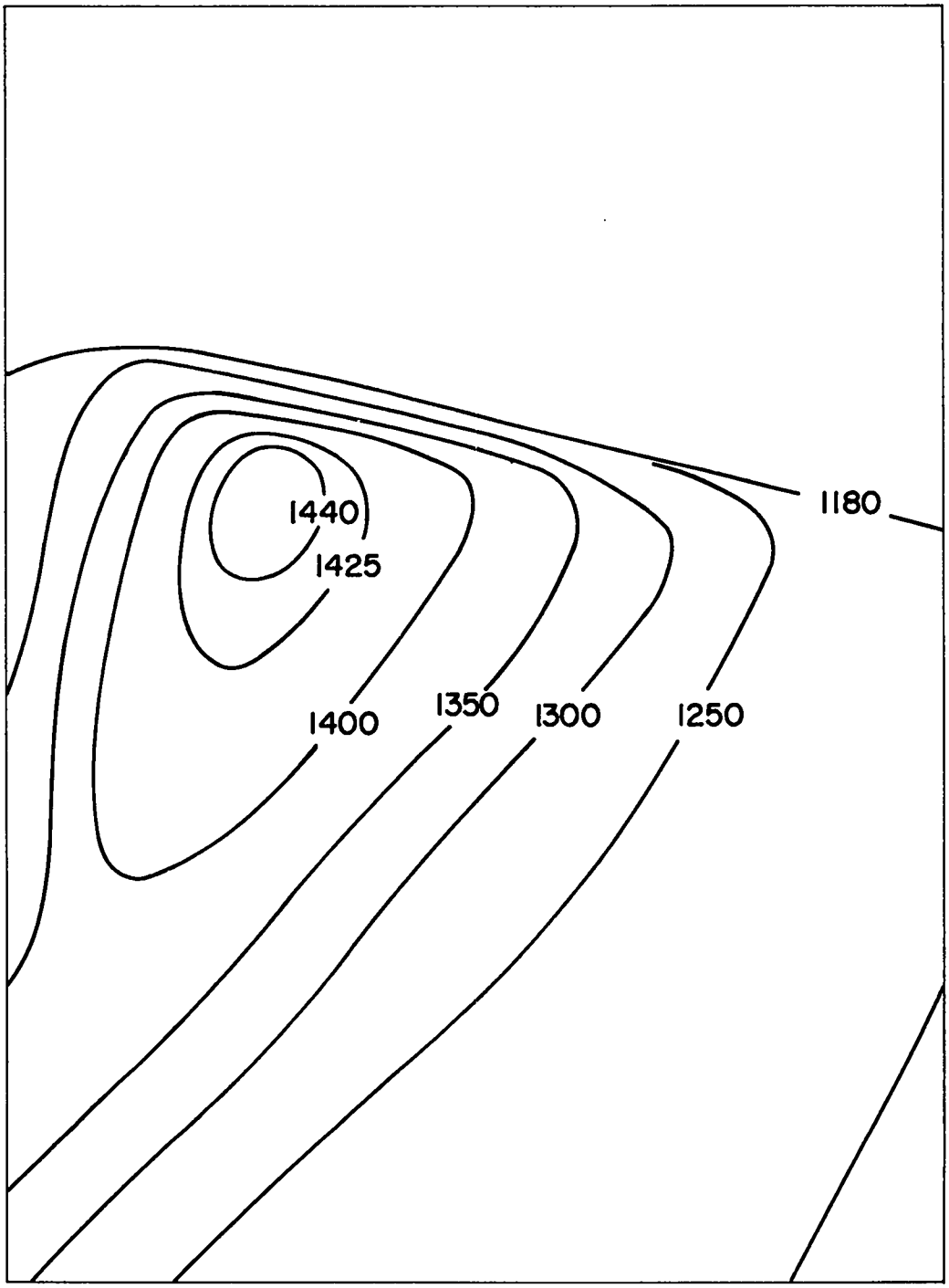

Fig. 5. The hot spot isotherms for the hot spot formed upon the interaction of a 96-kbar shock in Plexiglas with a nitromethane-filled corner formed by an aluminum plate perpendicular to a Plexiglas plate. The units are °K.

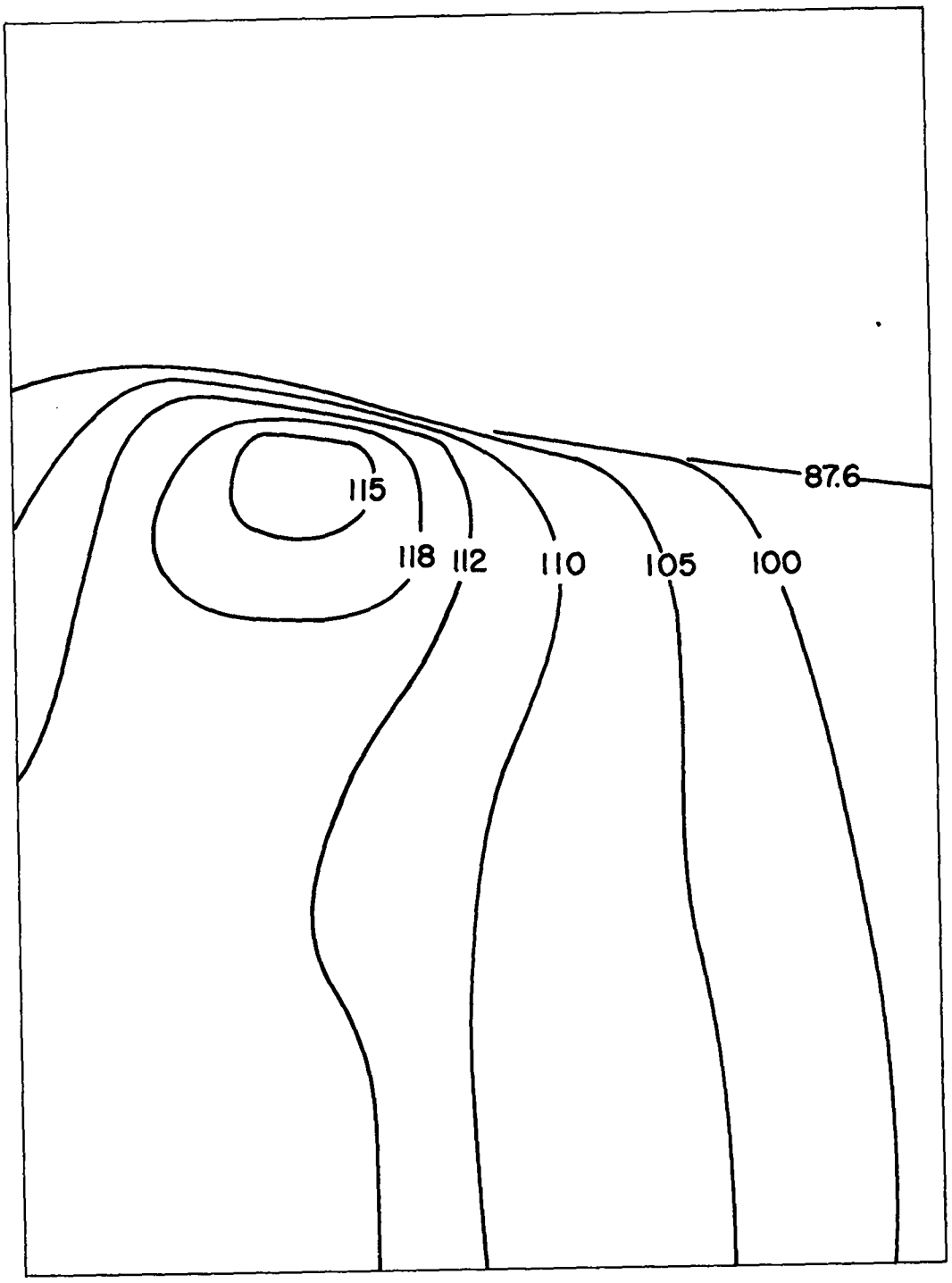

Fig. 6. The hot spot isobars for the hot spot formed upon the interaction of a 96-kbar shock in Plexiglas with a nitromethane-filled corner formed by an aluminum plate perpendicular to a Plexiglas plate. The units are kbars.

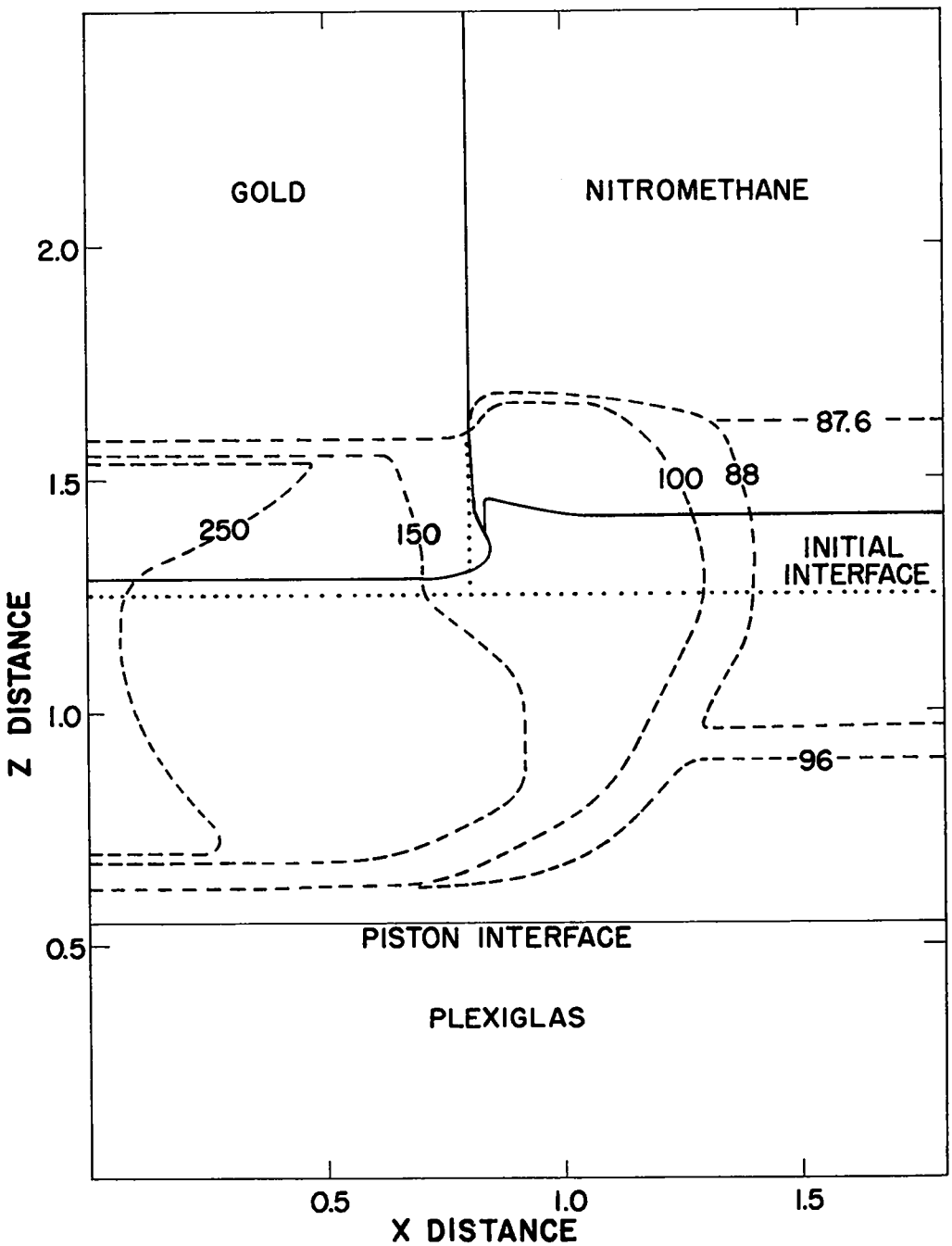

Fig. 7. The interface positions and isobars for the interaction of a 96-kbar shock in Plexiglas with a nitromethane-filled corner formed by a gold plate perpendicular to a Plexiglas plate. The interface position is shown by a solid line. The initial interface position is shown by a dotted line. The isobars are shown by dashed lines, and the units are kbars.

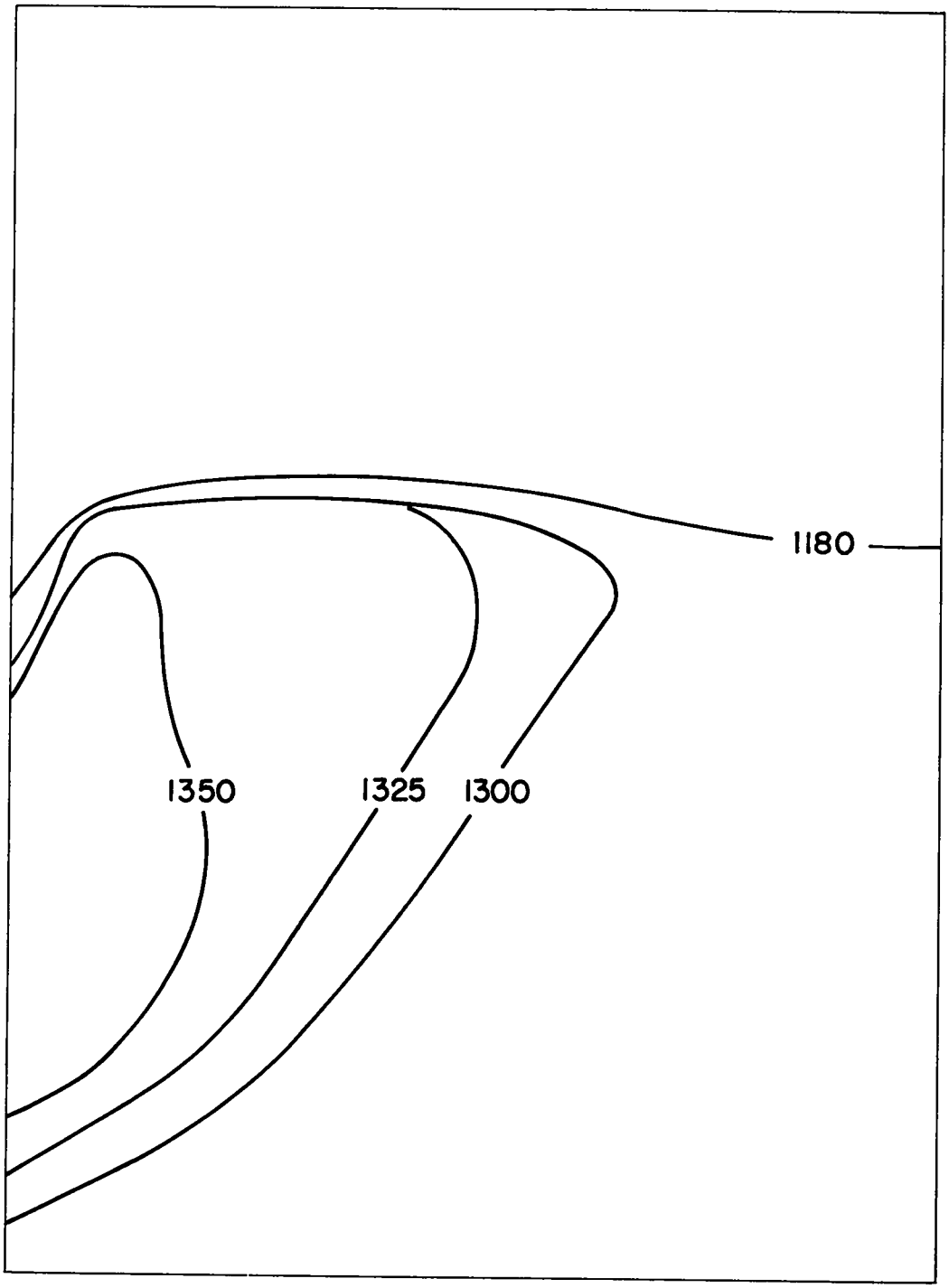

Fig. 8. The hot spot isotherms for the hot spot formed upon the interaction of a 96-kbar shock in Plexiglas with a nitromethane-filled corner formed by a gold plate perpendicular to a Plexiglas plate. The units are °K.

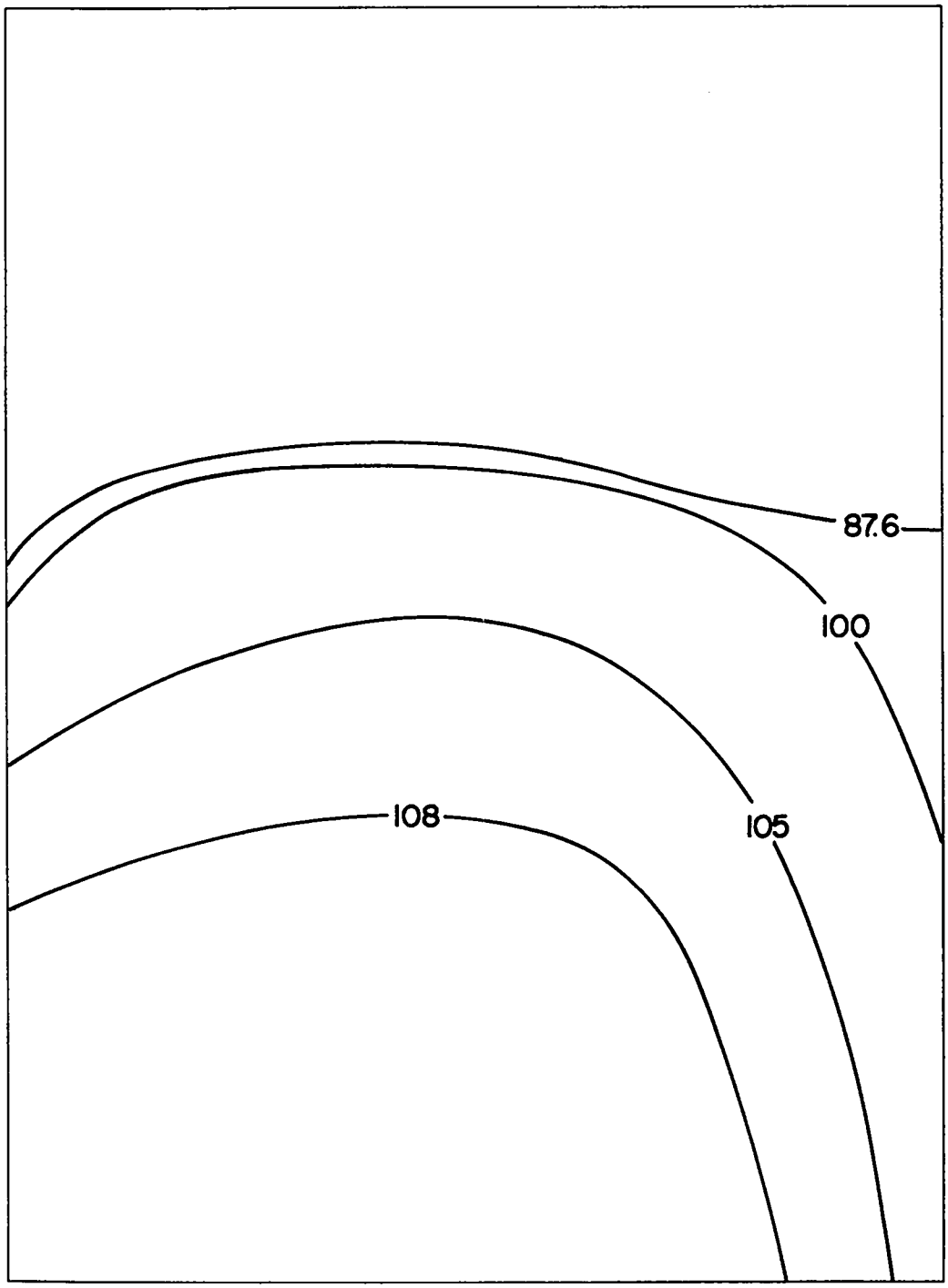

Fig. 9. The hot spot isobars for the hot spot formed upon the interaction of a 96-kbar shock in Plexiglas with a nitromethane-filled corner formed by a gold plate perpendicular to a Plexiglas plate. The units are kbars.

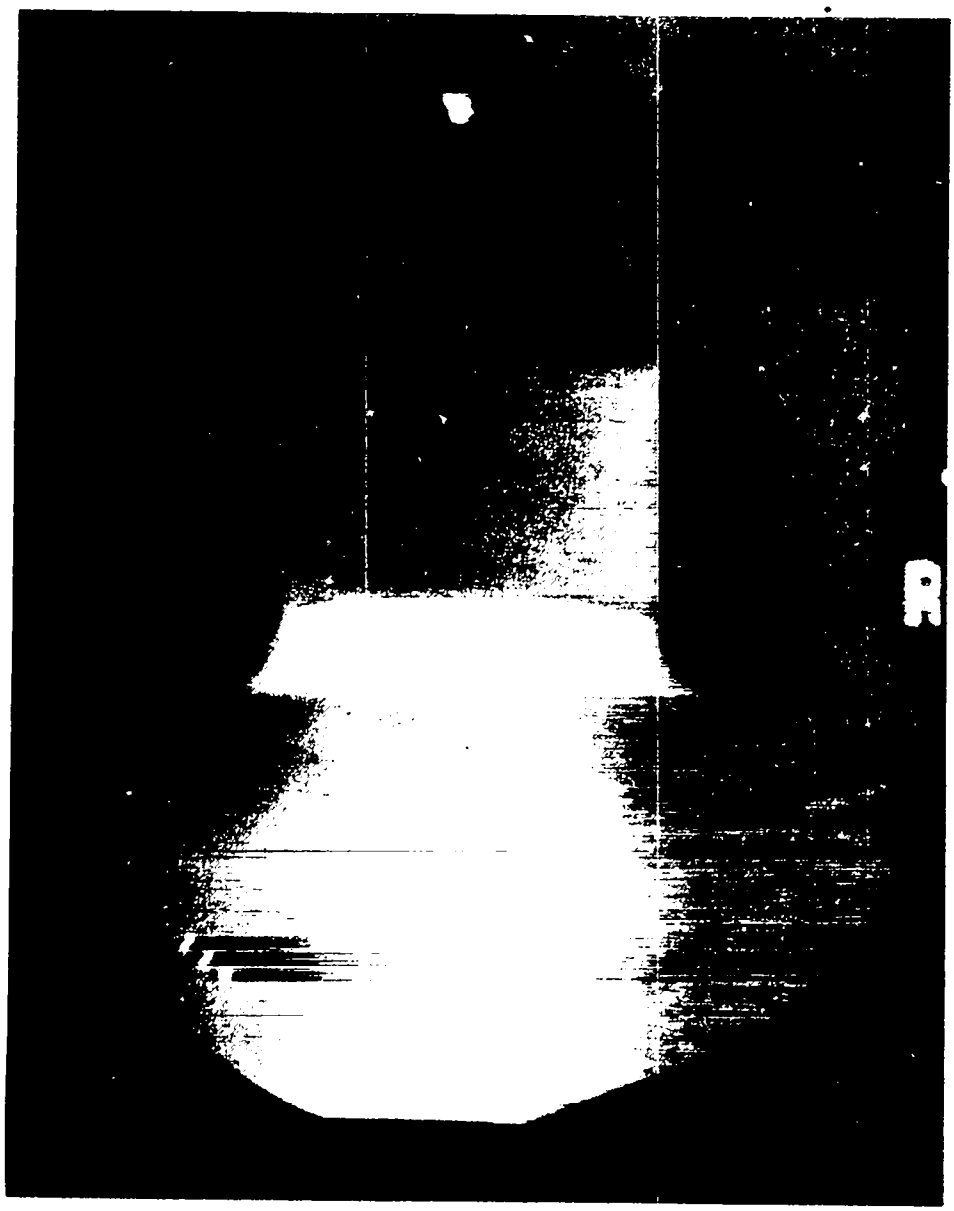

Fig. 10. The Phermex radiograph of the interaction of a 188-kbar shock in Plexiglas with a water-filled corner.

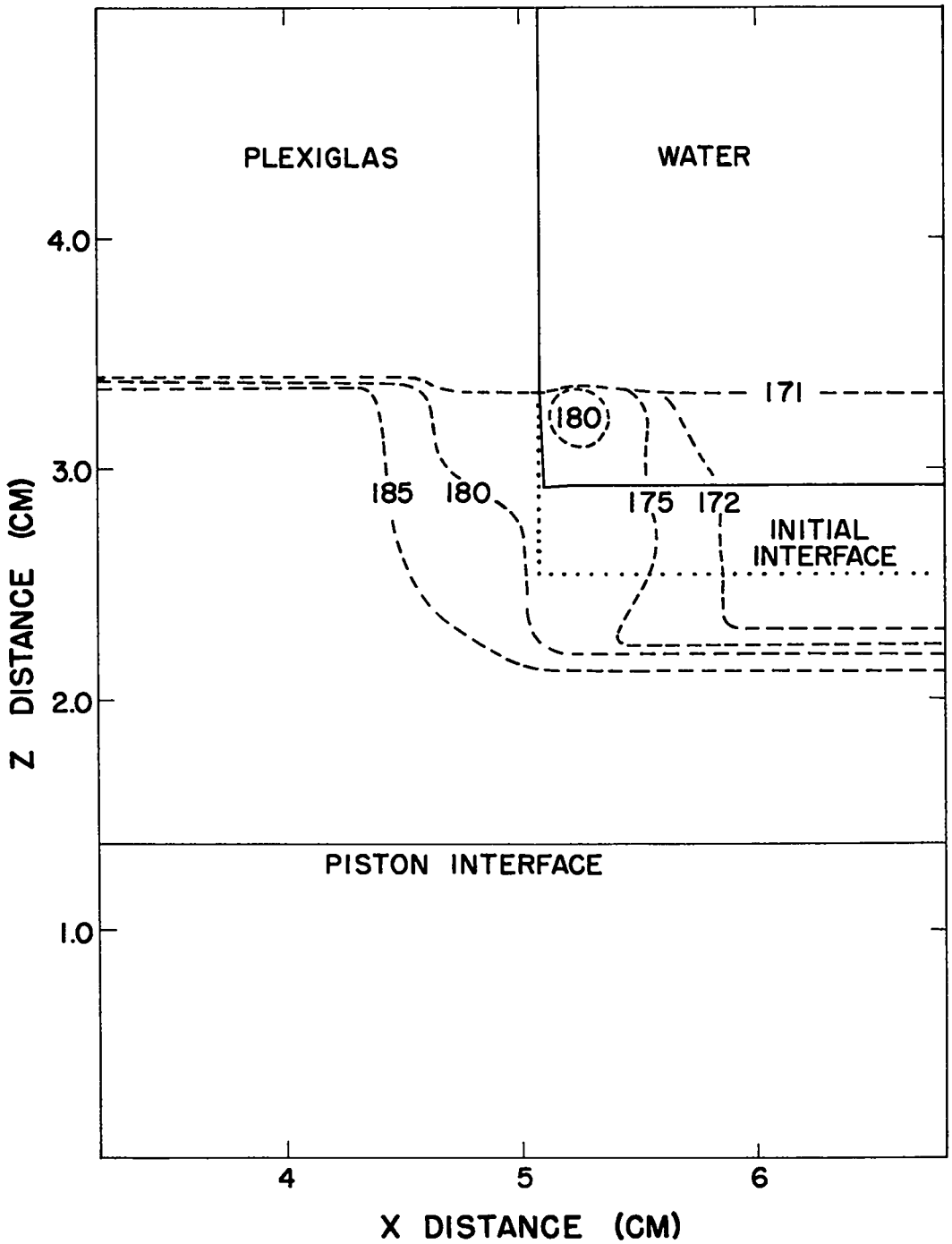

Fig. 11. The computed interface positions and isobars for the interaction of a 188-kbar shock in Plexiglas with a water-filled corner. The interface position is shown by a solid line. The initial interface position is shown by a dotted line. The isobars are shown by dashed lines, and the units are kbars.

APPENDIX A

THE HYDRODYNAMIC EQUATIONS

Many finite difference analogs of the Lagrangian equations of motion of a compressible fluid in two dimensions have been proposed. We used the "Magee" method developed and used during the last 15 years by group T-5 of the Los Alamos Scientific Laboratory. The "Magee" method has been described by Orr[5], Herrmann[6], Browne and Hoyt[7], and Kolsky[8]. We shall describe our version of the "Magee" method as coded in our 2DL code for the IBM 7030 and used to produce the numerical results described in this report.

The problem is divided into Lagrangian cells. At the intersections of the lines forming the Lagrangian cells are located the X and Z components of velocity (U_X, U_Z) and the coordinates of the intersections (X,Z). It is necessary to have N + 1 sets of velocity components and coordinates for each N cells. The rest of the cell quantities (P,T,W,M,I,V) are cell-centered, and it is necessary to have only N of each except that the cell mass has an extra boundary quantity.

The calculations are performed in three phases for each time step. The 2DL code performs each phase in order for all the cells in a block, proceeding in layers from cell X = 1, Z = 1 to cell X = N, Z = 1; then to cell X = 1, Z = 2; etc. The total number of cells is divided into blocks of X = 1-N, Z = 1-8; X = 1-N, Z = 9-16; etc. The blocks of quantities for the cells are kept on the disk with space for two blocks in the core memory. The calculation alternates between the two blocks in the core memory so as to overlap the transfer of data between the disk and core memory. One must save the last layer of the previous block for the beginning of the calculation of the present block. One must have the first layer of the next block before finishing the calculation of the last layer of the present block. The numerical calculations require sufficient time to permit the data transfer between the disk and

core memory to be overlapped.

The 2DL code can handle up to 62,000 cells and 7 components. Each floating point number in the STRETCH computer has three "flag bits" called T,U,V flags. The cell mass is flagged to describe which component a cell contains. The initial arrangement of the mesh generally requires a special routine for each problem, so a general purpose code cannot exist in the sense that the usual one-dimensional hydrodynamic codes are general purpose.

PHASE I

A. The quadrilateral cell is divided into two triangles.

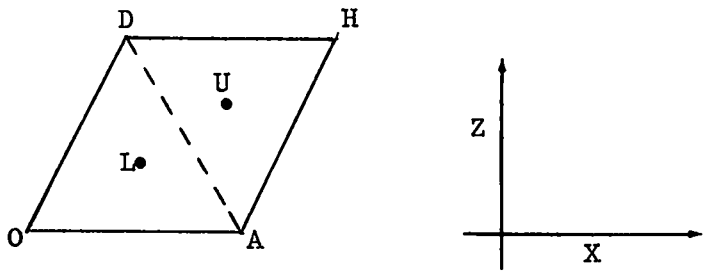

The areas of the triangles are

$$A_U = \tfrac{1}{2}\left[(Z_A - Z_H)(X_D - X_H) - (X_A - X_H)(Z_D - Z_H)\right]$$

$$A_L = \tfrac{1}{2}\left[(Z_D - Z_O)(X_A - X_O) - (X_D - X_O)(Z_A - Z_O)\right] .$$

The radii of the centroids are

$$\bar{X}_U = 1/3(X_H + X_D + X_A)$$

$$\bar{X}_L = 1/3(X_D + X_O + X_A) .$$

The specific volume of the cell is

$$V^{n+1} = \frac{A_L(\bar{X}_L)^{\alpha-1} + A_U(\bar{X}_U)^{\alpha-1}}{M} .$$

B. The energy of the cell is calculated from $dI = -PdV$, which in difference form is

$$I^{n+1} = I^n - \left(V^{n+1} - V^n\right)\left(P_1^n + q^n\right) .$$

C. Knowing I^{n+1}, V^{n+1}, and W^n, we use the HOM equation of state, described in Appendix B, to find P_1^{n+1}, T^{n+1}.

D. The artificial viscosity is calculated from $q = \frac{K^1}{V}\frac{\partial V}{\partial t}$, which in difference form is

$$q^{n+1} = \frac{K}{V^n}\left(V^{n+1} - V^n\right) .$$

If $(V^{n+1} - V^n) > 0$, then $q^{n+1} = 0$.

E. $P^{n+1} = P_1^{n+1} + q^{n+1}$; thus the viscous pressure is included in the following pressures.

F. Knowing T^{n+1} we calculate W^{n+1} using the Arrhenius rate law

$$\frac{dW}{dt} = Z^*We^{-E^*/R_gT} .$$

In difference form this is

$$W^{n+1} = W^n - \Delta t \; Z^* \; W^n \; e^{-E^*/R_gT^{n+1}} .$$

PHASE II

G. The accelerations are calculated using the force gradients method[5-7] which is derived at the end of this appendix.

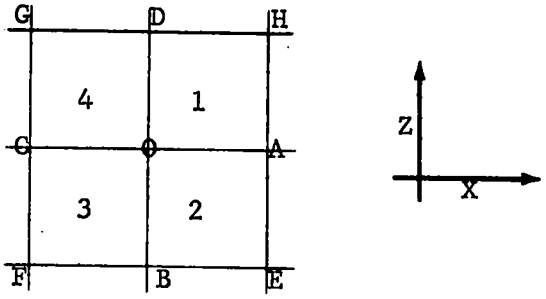

$$a_X = -\frac{(P_1 - P_4)(Z_D - Z_0)}{(M_1 + M_4)} \left(\left|\frac{X_D + X_0}{2}\right|\right)^{\alpha-1}$$
$$-\frac{(P_2 - P_3)(Z_0 - Z_B)}{(M_2 + M_3)} \left(\left|\frac{X_0 + X_B}{2}\right|\right)^{\alpha-1}$$
$$+\frac{(P_1 - P_2)(Z_A - Z_0)}{(M_1 + M_2)} \left(\left|\frac{X_A + X_0}{2}\right|\right)^{\alpha-1}$$
$$+\frac{(P_4 - P_3)(Z_0 - Z_C)}{(M_4 + M_3)} \left(\left|\frac{X_0 + X_C}{2}\right|\right)^{\alpha-1} .$$

$$a_Z = +\frac{(P_1 - P_4)(X_D - X_0)}{(M_1 + M_4)} \left(\left|\frac{X_D + X_0}{2}\right|\right)^{\alpha-1}$$
$$+\frac{(P_2 - P_3)(X_0 - X_B)}{(M_2 + M_3)} \left(\left|\frac{X_0 + X_B}{2}\right|\right)^{\alpha-1}$$
$$-\frac{(P_1 - P_2)(X_A - X_0)}{(M_1 + M_2)} \left(\left|\frac{X_A + X_0}{2}\right|\right)^{\alpha-1}$$
$$-\frac{(P_4 - P_3)(X_0 - X_C)}{(M_4 + M_3)} \left(\left|\frac{X_0 + X_C}{2}\right|\right)^{\alpha-1} .$$

H. The accelerations of the cells at the boundaries are computed separately using the above equations and the boundary conditions given below. The cells at boundaries are detected by testing on the cell pressure U flag. The type of boundary is determined from the flags of the cell energy as shown below.

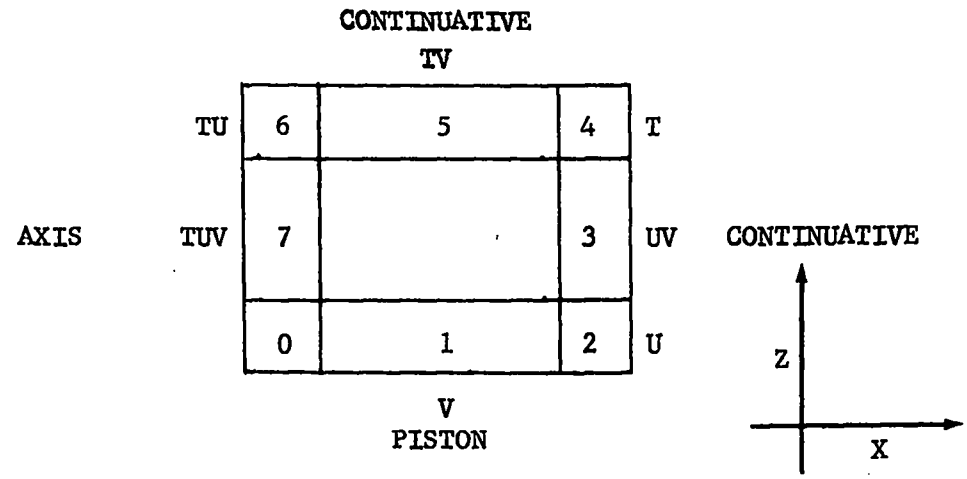

Flag	Boundary Conditions
0	$P_3, P_2 = P_{piston}$ $M_2, M_3, M_4 = M_1$ $P_4 = P_1$
	$X_C = -X_A$ $Z_B = 2Z_0 - Z_D$ $X_D, X_B, X_0 = 0$
1	$P_3, P_2 = P_{piston}$ $M_2 = M_1$ $M_3 = M_4$
	$X_B = X_D$ $Z_B = 2Z_0 - Z_D$
2	$P_3, P_2 = P_{piston}$ $M_3 = M_4$ $M_2 = M_1$ $P_1 = P_4$
	$X_B = X_D$ $Z_B = 2Z_0 - Z_D$ $Z_A = Z_C$ $X_A = 2X_0 - X_C$
3	$P_1 = P_4$ $P_2 = P_3$ $Z_A = Z_C$ $X_A = 2X_0 - X_C$
4	$P_2, P_1, P_4 = P_3$ $M_4 = M_3$ $M_1 = M_2$ $Z_A = Z_C$
	$X_A = 2X_0 - X_C$ $X_D = X_B$ $Z_D = 2Z_0 - Z_B$
5	$P_1 = P_2$ $P_4 = P_3$ $M_1 = M_2$ $M_4 = M_3$
	$X_D = X_B$ $Z_D = 2Z_0 - Z_B$

6 $P_3, P_4, P_1 = P_2 \quad M_3, M_4, M_1 = M_2 \quad X_D, X_B, X_O = 0$

$Z_D = 2Z_O - Z_B \quad Z_C = Z_A \quad X_C = -X_A$

7 $P_4 = P_1 \quad P_3 = P_2 \quad M_4 = M_1 \quad M_3 = M_2$

$Z_C = Z_A \quad X_C = -X_A \quad X_D, X_B, X_O = 0$

I. The cell particle velocities are calculated from

$$U_X^{n+1} = U_X^n + a_X \Delta t$$

$$U_Z^{n+1} = U_Z^n + a_Z \Delta t \ .$$

PHASE III

J. The cell boundary locations are calculated from

$$X^{n+1} = X^n + U_X^{n+1} \Delta t$$

$$Z^{n+1} = Z^n + U_Z^{n+1} \Delta t \ .$$

K. The total time is incremented by Δt, and the calculation starts again with Phase I.

THE "FORCE GRADIENTS" EQUATIONS

The following derivation of the "force gradients" equations for calculating the accelerations is almost identical to the derivation presented in reference 6.

In two dimensions, the conservation of mass and momentum may be expressed[6,8] as

$$\frac{\partial U_X}{\partial t} = a_X = -\frac{1}{\rho_0}\left(\frac{\partial P}{\partial X^1}\frac{\partial Z}{\partial Z^1} - \frac{\partial P}{\partial Z^1}\frac{\partial Z}{\partial X^1}\right)\left(\frac{X}{X^1}\right)^{\alpha-1}$$

$$\frac{\partial U_Z}{\partial t} = a_Z = -\frac{1}{\rho_0}\left(\frac{\partial P}{\partial Z^1}\frac{\partial X}{\partial X^1} - \frac{\partial P}{\partial X^1}\frac{\partial X}{\partial Z^1}\right)\left(\frac{X}{X^1}\right)^{\alpha-1} .$$

The Lagrangian gradients shown as the shaded zone may be expressed as

$$\left(\frac{\partial P}{\partial X^1}\right)_8 = \frac{P_1 - P_4}{X_1^1 - X_4^1}$$

$$\left(\frac{\partial Z}{\partial Z^1}\right)_8 = \frac{Z_D - Z_0}{Z_D^1 - Z_0^1} .$$

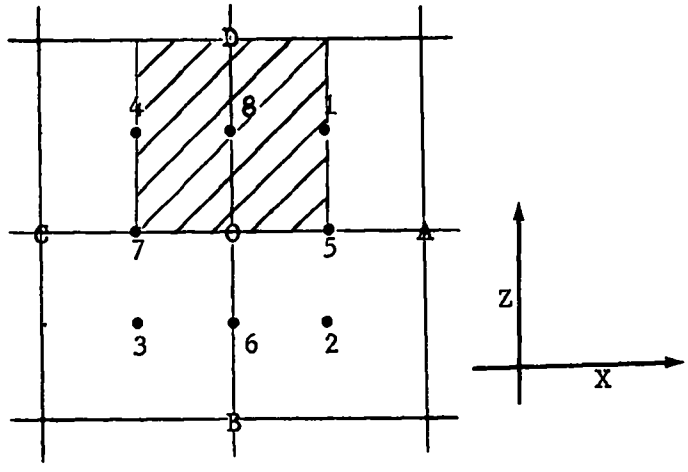

Writing similar expressions for zone 2 B 3 0, we can approximate the X gradient at 0 by

$$a_X = -\frac{1}{2\rho_0}\left[\frac{(P_1 - P_4)(Z_D - Z_0)}{(X_1^1 - X_4^1)(Z_D^1 - Z_0^1)}\left(\frac{\bar{X}}{\bar{X}^1}\right)_8^{\alpha-1} + \frac{(P_2 - P_3)(Z_0 - Z_B)}{(X_2^1 - X_3^1)(Z_0^1 - Z_B^1)}\left(\frac{\bar{X}}{\bar{X}^1}\right)_6^{\alpha-1}\right.$$

$$\left. - \frac{(P_1 - P_2)(Z_A - Z_0)}{(Z_1^1 - Z_2^1)(X_A^1 - X_0^1)}\left(\frac{\bar{X}}{\bar{X}^1}\right)_5^{\alpha-1} - \frac{(P_4 - P_3)(Z_0 - Z_C)}{(Z_4^1 - Z_3^1)(X_0^1 - X_C^1)}\left(\frac{\bar{X}}{\bar{X}^1}\right)_7^{\alpha-1}\right] .$$

Noting that

$$M_8 = \tfrac{1}{2}(M_1 + M_4) = \rho_0(X_1^1 - X_4^1)(Z_D^1 - Z_0^1)(\bar{X}^1)^{\alpha-1}, \text{ etc,}$$

and using the approximation $(\bar{X})_8 = \tfrac{1}{2}(X_D + X_0)$, etc, we obtain for the

acceleration in the X direction

$$a_X = - \frac{(P_1 - P_4)(Z_D - Z_0)}{(M_1 + M_4)} \left(\frac{X_D + X_0}{2} \right)^{\alpha-1}$$

$$- \frac{(P_2 - P_3)(Z_0 - Z_B)}{(M_2 + M_3)} \left(\frac{X_0 + X_B}{2} \right)^{\alpha-1}$$

$$+ \frac{(P_1 - P_2)(Z_A - Z_0)}{(M_1 + M_2)} \left(\frac{X_A + X_0}{2} \right)^{\alpha-1}$$

$$+ \frac{(P_4 - P_3)(Z_0 - Z_C)}{(M_4 + M_3)} \left(\frac{X_0 + X_C}{2} \right)^{\alpha-1} .$$

NOMENCLATURE

a_X	acceleration in X direction
a_Z	acceleration in Z direction
E*	activation energy
I	internal energy
K	constant used to compute artificial viscosity
M	cell mass/$(2\pi)^{\alpha-1}$ = $\rho_0 \Delta X \Delta Z$ for slabs; = $\left(X + \frac{\Delta X}{2}\right) \rho_0 \Delta X \Delta Z$ for cylinders (if cells are rectangular)
P	pressure
q	artificial viscosity
R_g	gas constant
T	temperature
U_X	particle velocity in X direction
U_Z	particle velocity in Z direction
V	specific volume
W	mass fraction of undecomposed explosive
X	spatial (Eulerian) coordinate in X direction
X^i	material (Lagrangian) coordinate in X direction
Z	spatial (Eulerian) coordinate in Z direction
Z^1	material (Lagrangian) coordinate in Z direction
α	= 1 for slab geometry; = 2 for cylindrical geometry
Δt	time increment
ρ	density

Superscript

n	the cycle number

Subscript

0	initial condition

APPENDIX B

THE EQUATION OF STATE

The Fickett and Wood[9] beta equation of state was chosen as the equation of state of the detonation products off the C-J isentrope. The pressure, volume, temperature, and energy values along the C-J isentrope were computed using the BKW equation of state[10-12] as recently calibrated by Mader[13]. The Grüneisen equation of state was used for the undetonated explosive off the experimental Hugoniot. Pressures and volumes on the Hugoniot are available from experimental data. Temperatures on the Hugoniot were calculated using the technique of Walsh and Christian[14]. The equation of state for mixtures of condensed explosive and detonation products was computed assuming pressure and temperature equilibrium.

THE HOM EQUATION OF STATE

Knowing I, V, W, calculate P, T.

A. Condensed component (If W = 1, then $I = I_s$, $V = V_s$).

For volumes smaller than V_o the experimental Hugoniot data are expressed as a linear fit of the shock and particle velocities. The temperatures are computed[15] using the technique of Walsh and Cristian[14].

$$(1) \qquad U_s = C + SU_p$$

$$P_H = \frac{C^2(V_o - V_s)}{\left[V_o - S\,(V_o - V_s)\right]^2}$$

$$(2) \qquad \ln T_H = F_s + G_s \ln V_s + H_s(\ln V_s)^2 + I_s(\ln V_s)^3 + J_s(\ln V_s)^4$$

$$(3) \qquad I_H = \tfrac{1}{2} P_H(V_o - V_s)$$

$$(4) \quad P_s = \frac{\gamma_s}{V_s} (I_s - I_H) + P_H \text{ where } \gamma_s = V\left(\frac{\partial P}{\partial I}\right)_V$$

$$(5) \quad T_s = T_H + \frac{(I_s - I_H)(23{,}890)}{C_V}$$

B. Gas component (detonation products, for example) (if W = 0, then $I = I_g$, $V = V_g$).

The pressure, volume, temperature, and energy of the detonation products along the C-J isentrope are computed using the BKW equation of state[12,13] and are fitted by the method of least squares to Equations (6) through (8).

$$(6) \quad \ln P_i = A + B\ln V_g + C(\ln V_g)^2 + D(\ln V_g)^3 + E(\ln V_g)^4$$

$$(7) \quad \ln I_i = K + L\ln P_i + M(\ln P_i)^2 + N(\ln P_i)^3 + O(\ln P_i)^4$$

$$I_i = I_i - Z \text{ (where Z is a constant used to change the standard state so as to be consistent with the condensed explosive standard state)}$$

$$(8) \quad \ln T_i = Q + R\ln V_g + S(\ln V_g)^2 + T(\ln V_g)^3 + U(\ln V_g)^4$$

$$(9) \quad -\frac{1}{\beta} = R + 2S\ln V_g + 3T(\ln V_g)^2 + 4U(\ln V_g)^3$$

$$(10) \quad P_g = \left(\frac{1}{\beta V_i}\right) (I_g - I_i) + P_i \text{ where } \beta = \frac{1}{V}\left(\frac{\partial I}{\partial P}\right)_V$$

$$(11) \quad T_g = T_i + \frac{(I_g - I_i)(23{,}890)}{C_V}$$

C. Mixture of condensed explosive and detonation products

$$(12) \quad V = WV_s + (1 - W)V_g$$

$$(13) \quad I = WI_s + (1 - W)I_g$$

$$(14) \quad P = P_g = P_s$$

$$(15) \quad T = T_g = T_s$$

The equation of state parameters and rate constants for nitromethane are given in Table I, and the sources of the data from which they were obtained are described in reference 16. The equation of state parameters for Plexiglas, aluminum, water, and gold are given in Table II. The data used to obtain the parameters are described in reference 17 for gold, in reference 14 for aluminum, and in reference 18 for water, and the data for Plexiglas are unpublished data obtained using the method described in reference 17.

NOMENCLATURE

C,S	constants in a linear fit of U_s and U_p
C_V	heat capacity of condensed component in cal/gm/deg
C_V'	heat capacity of gaseous component in cal/gm/deg
I	total internal energy in mb-cc/gm
P	pressure in megabars
T	temperature in °K
U_p	particle velocity
U_s	shock velocity
V	total volume in cc/gm
V_o	initial volume of condensed component in cc/gm
W	mass fraction of undecomposed explosive

Subscripts

g	gaseous component
H	Hugoniot
i	isentrope
s	condensed component

TABLE I. EQUATION OF STATE AND RATE PARAMETERS OF NITROMETHANE

Condensed		
C	+ 1.647	- 001
S	+ 1.637	+ 000
F_s	+ 5.41170789261	+ 000
G_s	- 2.72959322666	+ 000
H_s	- 3.21986013188	+ 000
I_s	- 3.90757138698	+ 000
J_s	+ 2.39028184133	+ 000
C_V	+ 4.14	- 001
α	+ 3.0	- 004
V_o	+ 8.86524823	- 001
γ_s	+ 0.6805	+ 000
T_o	+ 3.0	+ 002

Reaction		
E*	+ 5.36	+ 004
Z	+ 4.0	+ 008

BKW CJ Parameters		
P_{CJ}	+ 1.30	- 001
D_{CJ}	+ 6.463	- 001
T_{CJ}	+ 3.120	+ 003

Gas		
A	- 3.11585072896	+ 000
B	- 2.35968123302	+ 000
C	+ 2.10663268988	- 001
D	+ 3.80357006508	- 003
E	- 3.53454737231	- 003
K	- 1.39936678316	+ 000
L	+ 4.79350272379	- 001
M	+ 6.06707773429	- 002
N	+ 4.10672785525	- 003
O	+ 1.13326560531	- 004
Q	+ 7.79645302519	+ 000
R	- 5.33007196907	- 001
S	+ 7.09019736856	- 002
T	+ 2.06149976021	- 002
U	- 5.66139653675	- 003
C_V'	+ 5.56	- 001
Z	+ 1.0	- 001

TABLE II. EQUATION OF STATE PARAMETERS

	Plexiglas		Aluminum	
C	+ 2.43	- 001	+ 5.35	- 001
S	+ 1.5785	+ 000	+ 1.35	+ 000
F_s	+ 5.29380243506	- 001	+ 7.96115866874	+ 001
G_s	- 4.24950371368	+ 000	- 3.17533561633	+ 002
H_s	- 1.55055576332	+ 001	- 4.38525371533	+ 002
I_s	- 3.08638075572	+ 001	- 2.64248248960	+ 002
J_s	- 1.46708193739	+ 001	- 5.79734965732	+ 001
γ_s	+ 2.157	+ 000	+ 1.7	+ 000
C_v	+ 3.5	- 001	+ 2.2	- 001
α	+ 1.0	- 004	+ 2.4	- 005
V_o	+ 8.47457627000	- 001	+ 3.59066427289	- 001
	Water		Gold	
C	+ 2.264	- 001	+ 3.075	- 001
S	+ 1.325	+ 000	+ 1.56	+ 000
F_s	+ 5.69903609370	+ 000	+ 1.79784577873	+ 003
G_s	- 2.66572128557	- 001	+ 2.08878975374	+ 003
H_s	- 1.53713920377	+ 000	+ 8.97413382421	+ 002
I_s	- 7.58607109147	+ 000	+ 1.68445378136	+ 002
J_s	- 2.78464374578	+ 000	+ 1.16776763945	+ 001
γ_s	+ 1.65	+ 000	+ 2.12	+ 000
C_v	+ 1.0	+ 000	+ 3.12	- 002
α	+ 6.0	- 005	+ 1.42	- 005
V_o	+ 1.0	+ 000	+ 5.19750519751	- 002

LITERATURE CITED

1. Mader, Charles L., "The Two-Dimensional Hydrodynamic Hot Spot", Los Alamos Scientific Laboratory report LA-3077 (1964).

2. Mader, Charles L., "The Two-Dimensional Hydrodynamic Hot Spot, Volume II", Los Alamos Scientific Laboratory report LA-3235 (1964).

3. Mader, Charles L., "Initiation of Detonation by the Interaction of Shocks with Density Discontinuities", Phys. Fluids 8, 1811 (1965).

4. Travis, J. R., "Experimental Observations of Initiation of Nitromethane by Shock Interactions at Discontinuities", Preprints of the Fourth Symposium on Detonation, C-45 (1965).

5. Orr, S. R., "F Magee", Los Alamos Scientific Laboratory Unpublished Note, 1961.

6. Herrmann, W., "Comparison of Finite Difference Expressions Used in Lagrangian Fluid Flow Calculations", Air Force Weapons Laboratory, Kirtland Air Force Base, New Mexico, report WL-TR-64-104 (1964).

7. Browne, Phillip L. and Hoyt, Martha S., "HASTI - A Numerical Calculation of Two-Dimensional Lagrangian Hydrodynamics Utilizing the Concept of Space-Dependent Time Steps", Los Alamos Scientific Laboratory report LA-3324-MS (1965).

8. Kolsky, H. G., "A Method for the Numerical Solution of Transient Hydrodynamic Shock Problems in Two Space Dimensions", Los Alamos Scientific Laboratory report LA-1867 (1955).

9. Fickett, W., and Wood, W. W., "A Detonation-Product Equation of State Obtained From Hydrodynamic Data", Phys. Fluids 1, 528 (1958).

10. Cowan, R. D., and Fickett, W., "Calculation of the Detonation Properties of Solid Explosives with the Kistiakowsky-Wilson Equation of State", J. Chem. Phys. 24, 932 (1956).

11. Mader, Charles L., "Detonation Performance Calculations Using the Kistiakowsky-Wilson Equation of State", Los Alamos Scientific Laboratory report LA-2613 (1961).

12. Mader, Charles L., "STRETCH BKW - A Code for Computing the Detonation Properties of Explosives", Los Alamos Scientific Laboratory report LADC-5691 (1962).

13. Mader, Charles L., "Detonation Properties of Condensed Explosives Computed Using the Becker-Kistiakowsky-Wilson Equation of State", Los Alamos Scientific Laboratory report LA-2900 (1963).

14. Walsh, John M., and Christian, Russell H., "Equation of State of Metals From Shock Wave Measurements", Phys. Rev. 97, 1544 (1955).

15. Mader, Charles L., "STRETCH SIN - A Code for Computing One-Dimensional Reactive Hydrodynamic Problems", Los Alamos Scientific Laboratory report TID-18571 or LADC-5795 (1963).

16. Mader, Charles L., "The Hydrodynamic Hot Spot and Shock Initiation of Homogeneous Explosives", Los Alamos Scientific Laboratory report LA-2703 (1962).

17. McQueen, R. G. and Marsh, S. P., "Equation of State for Nineteen Metallic Elements from Shock-Wave Measurements to Two Megabars", J. Appl. Phys. 31, 1253 (1960).

18. Walsh, J. M. and Rice, M. H., "Dynamic Compression of Liquids from Measurements on Strong Shock Waves", J. Chem. Phys. 26, 815 (1957).